ARTICLE
Journal of Cellular Biochemistry 113:3093–3103 (2012)

Journal of Cellular Biochemistry

Alternation of Extracellular Matrix Remodeling and Apoptosis by Activation of the Aryl Hydrocarbon Receptor Pathway in Human Periodontal Ligament Cells

Atsushi Tomokiyo, Hidefumi Maeda,* Shinsuke Fujii, Satoshi Monnouchi, Naohisa Wada, Kiyomi Hori, Katsuaki Koori, Naohide Yamamoto, Yoko Teramatsu, and Akifumi Akamine

Faculty of Dental Science, Division of Oral Rehabilitation, Department of Endodontology and Operative Dentistry, Kyushu University, 3-1-1 Maidashi, Higashi-ku, Fukuoka 812-8582, Japan

ABSTRACT

It is well known that the aryl hydrocarbon receptor (AhR) is involved in the toxicity of halogenated aromatic hydrocarbons (HAH) and polycyclic aromatic hydrocarbons (PAH). Recent experiments have shown the induction of impaired tooth and hard-tissue formation by AhR pathway activation, however, the effect on periodontal ligament (PDL) tissue remains unclear. Here, we investigated the effects of benzo(a)pyrene (BaP), a member of PAH, on the extracellular matrix (ECM) remodeling-related molecules, collagen type I (COL-I), matrix metalloproteinase-1 (MMP-1), alpha-smooth muscle actin (α-SMA) expression, and apoptosis in two different human periodontal ligament cells (HPDLCs). The transduction of AhR from the cytoplasm to the nucleus and the increase of AhR-responsive genes; that is, *cytochrome P450 1A1* (*CYP1A1*), *cytochrome P450 1B1* (*CYP1B1*), and *aryl-hydrocarbon receptor repressor* (*AhRR*), expression was induced by BaP exposure in both HPDLCs. BaP treatment significantly enhanced *MMP-1* mRNA expression and MMP-1 protein production, while markedly suppressing *COL-I* and *a-SMA* mRNA expression in both HPDLCs. Furthermore, these BaP-treated HPDLCs fell into apoptotic cell death as evidenced by induction in annexin V and caspase-3/7 staining and reduction of total cell number and *Bcl-2* mRNA expression. Thus, BaP exposure altered the expression of ECM-related molecules and induced apoptosis in HPDLCs through activation of the AhR pathway. Overactivity of the AhR pathway may induce an inappropriate turnover of PDL tissue via disordered ECM remodeling and apoptosis in PDL cells. J. Cell. Biochem. 113: 3093–3103, 2012.

KEY WORDS: PERIODONTAL LIGAMENT; ARYL HYDROCARBON RECEPTOR; MATRIX METALLOPROTEINASE-1; COLLAGEN TYPE I; ALPHA-SMOOTH MUSCLE ACTIN

Halogenated aromatic hydrocarbons (HAH) and polycyclic aromatic hydrocarbons (PAH) are widely spread environmental pollutants that toxically affect a variety of organs and cells. It is generally accepted that their toxic effects are directly mediated through aryl hydrocarbon receptor (AhR) pathway activation [Nebert et al., 2000]. AhR is a ligand-activated cytosolic protein, which belongs to a family of transcriptional regulatory proteins containing the basic helix-loop-helix/Per-Arnt-Sim (bHLH/PAS) domain structure, with multiple functions in metabolism and development [Gu et al., 2000]. Previous reports have demonstrated the diverse effects of AhR pathway activation on acute and chronic toxicity, such as immunosuppression, thymic atrophy, teratogenesis, carcinogenesis, and developmental defects [Pohjanvirta and Tuomisto, 1994]. AhR pathway activation was revealed to elicit impaired tooth and hard-tissue formation. In rats, the most toxic congener of HAH, 2,3,7,8-tetrachlorodibenzo-*p*-dioxin (TCDD), induced apoptosis of dental epithelial cells, reduced tooth size, and deformed cuspal morphology [Partanen et al., 2004]. TCDD exposure also enhanced caries susceptibility and inhibited third molar formation [Kattainen et al., 2001]. In humans, the exposure to high amounts of HAH revealed missing permanent teeth (Alaluusua and Lukinmaa, 2000). Dietary exposure to HAH also induced

Grant sponsor: Ministry of Education, Culture, Sports, Science, and Technology, Japan; Grant numbers: 21390510, 21791942, 22390359, 23659890, 23689077.

*Correspondence to: Hidefumi Maeda, DDS, PhD, Faculty of Dental Science, Division of Oral Rehabilitation, Department of Endodontology and Operative Dentistry, Kyushu University, 3-1-1 Maidashi, Fukuoka 812-8582, Japan. E-mail: hide@dent.kyushu-u.ac.jp

Manuscript Received: 5 April 2012; Manuscript Accepted: 2 May 2012

Accepted manuscript online in Wiley Online Library (wileyonlinelibrary.com): 11 May 2012

DOI 10.1002/jcb.24186 • © 2012 Wiley Periodicals, Inc.

developmental enamel defects, demarcated opacities, and hypoplasia [Jan and Vrbic, 2000]. Moreover, the Yusho patients accidentally exposed to a high level of HAH-related compounds via ingestion of contaminated rice oil sometimes showed horizontal alveolar bone resorption and deep periodontal pockets, despite good dental plaque control [Shimizu et al., 1992]. However, the effects of AhR pathway activation on periodontal ligament (PDL) cells have not been fully examined.

Benzo(a)pyrene (BaP) is an important and extensively studied member of the PAH. Its cytotoxic, carcinogenic, and mutagenic effects have been well documented in various animal species. Sources of BaP include automobile emissions, industrial processes, tobacco smoke, incineration facilities, and hazardous waste sites [Wu et al., 2003]. In the first step of metabolism, BaP binds to AhR and the liganded AhR translocates to the nucleus, where it forms a heterodimer with ARNT [Rowlands and Gustafsson, 1997].

The PDL is a highly specialized connective tissue that surrounds the root of the tooth and connects it with the tooth socket bone [Carnes et al., 1997]. Apart from anchoring the tooth, the PDL tissue also ensures proper tooth homeostasis, repair, nutrition, and sensory transmission [Shimono et al., 2003]. Once PDL tissue is severely destroyed, the periodontium exhibits common clinical symptoms such as deep periodontal pocket formation, extensive alveolar bone loss, necrotic or exposed cementum development, and high tooth mobility. The final stage of PDL destruction is characterized by tooth loss.

PDL tissue consists of a heterogeneous cell population, including fibroblasts, mesenchymal stem cells, epithelial cell rests of Malassez, and endothelial cells [Freeman, 1994]. These cells are embedded in a protein-rich extracellular matrix (ECM) that is constantly remodeled in response to various types of stimulation. The periodontal ECM is composed of both collagenous and non-collagenous proteins. Collagens in PDL tissue are divided into three groups: the fibril-forming collagens (collagen type I [COL-I], collagen type-III [COL-III] and collagen type-V [COL-V]), the non-fibril-forming collagens (collagen type- VI [COL-VI]), and the fibril-associated collagens with interrupted triple helices (collagen type-XII [COL-XII] and collagen type-XIV [COL-XIV]) [Nemoto et al., 2010]. Among them, COL-I is a major collagen and plays a crucial role in protecting PDL tissue from mechanical stress, such as masticatory loading [Butler et al., 1975]. Alpha-smooth muscle actin (α-SMA), an actin isoform typical of vascular smooth muscle cells, is also known to be important for contractile force generation by fibroblasts [Skalli et al., 1986]. α-SMA is known as a putative marker of myofibroblastic cells and is important for myofibroblast differentiation, focal adhesion maturation, and force generation [Desmouliere et al., 2005]. In addition, Lekic et al. [2001] revealed that the high percentages of PDL cells express α-SMA in vivo and in vitro. Matrix remodeling and collagen turnover have been known to be very rapid in PDL tissue [Sodek and Limeback, 1979]. Matrix metalloproteinases (MMPs) belong to a family of zinc-dependent enzymes that are responsible for degradation of fibrillar collagen and other ECM proteins [Galis et al., 1994]. In PDL tissue, MMPs play a central role in ECM remodeling, both in physiological and in pathological conditions [Kerrigan et al., 2000]. Presently, at least 28 MMPs have been identified, among which MMP-1 is capable of degrading interstitial COL-I, -II, and -III. MMP-1 is constitutively synthesized by many different cell types including PDL cells [Alvares et al., 1995].

In most tissues, the biological processes of cell proliferation, differentiation, and apoptosis are all tightly coupled to appropriate alterations in metabolic status and their imbalance promotes tissue destruction. Previous reports demonstrated the involvement of apoptosis in the development of various oral diseases including periodontal disease [Loro et al., 2005]. A number of physiological and pathological stimuli including lack of nutrients, activation of cell surface death receptors, chemicals, ionizing radiation, and direct physical injury can activate the apoptotic pathways. In PDL cells, several toxic factors such as leukotoxins, lipoproteins, lipopolysaccharides, and hydrogen sulfide induced apoptosis (Zhang et al., 2010).

The aim of this study was to investigate the effects of AhR pathway activation on PDL tissue remodeling and apoptosis. Here, we report that BaP activated the AhR pathway in two different human periodontal ligament cells (HPDLCs) in a similar manner. In addition, BaP treatment promoted *MMP-1* mRNA expression, MMP-1 protein production and apoptosis, and suppressed *COL-I* and *α-SMA* mRNA expression in both HPDLCs.

MATERIALS AND METHODS

CELL CULTURE

HPDLCs, reported in our previous studies, were used [Fujii et al., 2006; Maeda et al., 2011]. Briefly, the cells were isolated from healthy premolars or third molars of six different patients, two 30-year-old females (2D and 2G), a 14-year-old male (2I), a 22-year-old female (3D), a 26-year-old male (3M), a 20-year-old female (3O) who visited Kyushu University Hospital for extraction. The keratinocyte cell line, HaCaT, was kindly provided by N. E. Fusenig, DKFZ Heidelberg (Boukamp et al., 1988). This line was used as a positive control for the ligand-activated AhR pathway. HPDLCs-2D, -2G, -2I, -3D, -3M, -3O, and HaCaT were maintained in α-minimum essential medium (α-MEM; Gibco-BRL, Grand Island, NY) supplemented with 50 μg/ml streptomycin and 50 U/ml penicillin (Gibco-BRL) containing 10% fetal bovine serum (FBS; SAFC Bioscience, Lenexa, KS; 10% FBS/α-MEM) in a humidified atmosphere of 5% CO_2 and 95% air at 37°C. All procedures were performed in compliance with the Research Ethics Committee, Faculty of Dentistry, Kyushu University.

SEMI-QUANTITATIVE RT-PCR

HPDLCs-2D, -2G, -2I, -3D, -3M, -3O, or HaCaT were seeded in 60 mm dishes (1×10^5 cells/dish) in 10% FBS/α-MEM containing 0.01% dimethyl sulfoxide (Wako, Osaka, Japan) as control medium (CM). After 24 h, total cellular RNA was extracted using TRIzol Reagent (Invitrogen, Carlsbad, CA). First-strand cDNA synthesis and semi-quantitative PCR were performed as described previously [Fujii et al., 2008]. Primer sequences, annealing temperatures, cycle numbers, and product sizes for each gene are listed in Table I. The mRNA expression levels were evaluated by densitometric image analysis using Scion Image Software (Scion Corporation, Walkersville, MD).

TABLE I. Specific Primer Sequence, Annealing Temperature, Cycle Numbers, and Product Size for Semi-Quantitative RT-PCR

Target gene (abbreviation)	Primer sequence forward/reverse	Annealing temperature (°C)	Cycles	Size of amplified products (bp)
Aryl hydrocarbon receptor (AhR)	5′-TACTGAAGCAGAGCTGTGCA-3′/5′-CTCATACAACACAGCTTCTCC-3′	58	24	315
Glyceraldehyde-3-phosphate dehydrogenase (GAPDH)	5′-ACCACAGTCCATGCCATCCAC-3′/5′-TCCACCACCCTGTTGCTGTA-3′	60	17	452

IMMUNOCYTOCHEMICAL STAINING

HPDLCs-2D, -2G, -2I, -3D, -3M, -3O, and HaCaT, cultured for 24 h, in CM were fixed with 4% paraformaldehyde including 0.5% dimethyl sulfoxide in phosphate-buffered saline (PBS; Gibco-BRL) for 20 min. After blocking in 5% skim milk (Yukijirushi, Hokkaido, Japan) containing 0.01% NaN_3 (Nacalai Tesque, Kyoto, Japan) in PBS for 1 h, a rabbit polyclonal anti-human AhR (AbD Serotec, Oxford, UK; 1:100) was applied for 2 h. Cells were rinsed with PBS and exposed to a biotinylated secondary antibody and avidin-peroxidase conjugate using a SAB-PO kit (Nichirei, Tokyo, Japan). For color development, cells were treated with 3,3′-diaminobenzidine (DAB; Nichirei). Cells were observed with an inverted microscope (BX41; Olympus Medical, Tokyo, Japan). HPDLCs-2G, cultured for 4 days in CM or CM + 10 μM benzo(a)pyrene (BaP; Sigma, St. Louis, MO) was also stained with a rabbit polyclonal anti-human AhR (1:100). Following washing with PBS, cells were exposed to a goat FITC-labeled anti-rabbit (Zymed, South San Francisco, CA; 1:20). After 1 h, cells were washed with PBS and counterstained with VECTASHIELD Mounting Medium with DAPI (Vector Laboratories, Burlingame, CA). Cells were observed with fluorescence microscopy (AXIOPLAN; Carl Zeiss, Jena, Germany). The alternating dishes from each experimental condition were processed with blocking solution as a negative control with no primary antibody.

QUANTITATIVE RT-PCR

HPDLCs-2G, -2I, or HaCaT were cultured in 60 mm dishes (1×10^5 cells/dish) for 24 h or 14 days in CM, CM + 1 μM BaP, or CM + 10μM BaP. In addition, HPDLCs-2G or -2I were incubated for 20, 40, or 60 min or 0, 14, or 28 days in CM or CM + 10 μM BaP. Following total cellular RNA extraction and first-strand cDNA synthesis, quantitative PCR was performed [Tomokiyo et al., 2008; Maeda et al., 2011]. Primer sequences, annealing temperatures, cycle numbers, and product sizes for each gene are listed in Table II.

ENZYME-LINKED IMMUNOSORBENT ASSAY (ELISA)

To quantify the concentration of MMP-1 protein secreted from HPDLCs, a sensitive two-site ELISA was performed. HPDLCs-2G or -2I were seeded at 5×10^5 cells/dish on a 100 mm dish in CM or CM + 10 μM BaP. After 7 or 14 days, the confluent cells were thoroughly washed with PBS and incubated in serum-free α-MEM. After 24 h, the conditioned media from these cells were collected. A commercially available ELISA kit (Quantikine Human pro-MMP-1 Immunoassay; R&D Systems, Minneapolis, MN) was used to quantify the MMP-1 concentration in these conditioned media. The absorbance was measured at 450 nm with Immuno-mini NJ-2300 (Microtec, Chiba, Japan). All samples and standards were measured in triplicate.

CELL VIABILITY

HPDLC-2G or -2I were seeded at 1×10^3 cells/well on 48-well plates in CM, CM + 1 μM BaP, or CM + 10μM BaP. Four wells were assigned to each experimental treatment. Following the 3, 5, or 7 days culture, adherent cells were detached with 0.05% trypsin (Wako) containing 0.02% ethylenediaminetetraacetic acid (Wako) in PBS. After centrifugation at 1,100 rpm for 5 min, the solution was removed by aspiration. Then, cells were resuspended in α-MEM and 10 μl cell suspension was used for direct cell count. The number of cells was estimated using a BX41 inverted microscope and a hemocytometer. HPDLC-2G or -2I were seeded at 5×10^5 cells/dish

TABLE II. Specific Primer Sequence, Annealing Temperature, Cycle Numbers, and Product Size for Quantitative RT-PCR

Target gene (abbreviation)	Primer sequence forward/reverse	Annealing temperature (°C)	Cycles	Size of amplified products (bp)
Cytochrome P450 1A1 (CYP1A1)	5′-TGGTCTCCCTTCTCTACACTCTTGT-3′/5′-ATTTTCCCTATTACATTAAATCAATGGTTCT-3′	60	40	141
Cytochrome P450 1B1 (CYP1B1)	5′-CCTATGTCCTGGCCTTTCCTTT-3′/5′-TGAGGAATAGTGACAGGCACAAA-3′	60	40	67
Aryl-hydrocarbon receptor repressor (AhRR)	5′-GCCTCTGGGCATTTATGGATTTAAG-3′/5′-CTGGGCACTCGGTTAGAATAGGAA-3′	60	40	82
Matrix metalloproteinase-1 (MMP-1)	5′-CTGGCCCACAACTGCCAAATG-3′/5′-CTGTCCCTGAACAGCCCAGTACTTA-3′	60	40	103
Collagen type 1 (COL-1)	5′-CCCGGGTTTCAGAGACAACTTC-3′/5′-TCCACATGCTTTATTCCAGCAATC-3′	60	40	148
Alpha-smooth muscle actin (α-SMA)	5′-GACAATGGCTCTGGGCTCTGTAA-3′/5′-CTGTGCTTCGTCACCCACGTA-3′	60	40	147
Bcl-2	5′-TGGGATGCCTTTGTGGAACT-3′/5′-GAGACAGCCAGGAGAAATCAAAC-3′	60	40	67
β-actin (β-ACT)	5′-ATTGCCGACAGGATGCAGA-3′/5′-GAGTACTTGCGCTCAGGAGGA-3′	60	40	89

on a 100 mm dish in CM or CM + 10 μM BaP. Following the 3 or 24 h culture, adherent cells were detached with trypsin. Then, for detection of apoptotic cells, double labeling for annexin V and propidium iodide (PI) was performed using an annexin V FITC kit (Miltenyi Biotec Inc., Auburn, CA). The percentage of apoptotic cells was measured on a FACSCalibur and analyzed with CellQuest software (Becton Dickinson Labware, Lincoln Park, NJ). HPDLCs-2G or -2I were also seeded at 5×10^5 cells/dish on a 100 mm dish in CM. After 3 days, the cells were detached by trypsin and incubated with CM or CM + 10 μM BaP at 5×10^5 cells/ml in 15 ml polypropylene culture tubes (Sumilon, Tokyo, Japan). After 24 h, the expression of active caspase-3/7 in suspended cells was detected with a FLICA Apoptosis Detection Kit (Immunochemistry Technologies, LLC, Bloomington, MN), which contained a green fluorescent-labeled inhibitor of activated caspases, FAM-DEVD-FMK FLICA. This probe binds covalently to active caspase-3/7 in apoptotic cells. Following counterstaining with Hoechst (Immunochemistry Technologies, LLC), cells were observed by fluorescence microscopy (Carl Zeiss). All samples were measured in duplicate.

STATISTICAL ANALYSIS

Each experimental value represents the mean ± SD. Independent repeats were performed at least twice and four different replicates were analyzed for all experiments. Statistical significance was determined using Student's *t*-test, and $P < 0.05$ was considered significant.

RESULTS

EXPRESSION OF AhR IN HPDLCs AND HaCaT

A previous study showed the endogenous expression of AhR in a human keratinocyte cell line, HaCaT [Ikuta et al., 2004]. Therefore, we first investigated the expression of *AhR* mRNA in HPDLCs-2D, -2G, -2I, -3D, -3M, -3O, and HaCaT cultured in CM for 24 h by semi-quantitative RT-PCR analysis. In agreement with the previous result, HaCaT expressed *AhR* mRNA (Fig. 1A). In addition, the expression level of HaCaT was almost similar to that of HPDLCs (Fig. 1A). Next, we performed immunocytochemical staining with anti-human AhR antibodies for HPDLCs-2D, -2G, -2I, -3D, -3M, -3O, and HaCaT. As shown in Figure 1B, intracellular distribution of AhR was confirmed in nearly all cells. Higher magnification images exhibited strongly positive staining in the cytoplasm in HPDLCs and HaCaT while staining was faint in their nuclei (Fig. 1C,E-J). Staining without a primary antibody did not reveal any positive reactions (Fig. 1D).

ACTIVATION OF THE AhR PATHWAY IN HPDLCs

In Figure 1A, all of six HPDLCs expressed *AhR* mRNA and its expression level was relatively low in HPDLCs-2G, while relatively high in HPDLCs-2I. Therefore, we selected HPDLCs-2G and 2I to examine the effects of AhR pathway activation of HPDLCs. The cellular localization of AhR was investigated in HPDLCs-2G cultured for 4 days in CM or CM + 10 μM BaP. The cells cultured in CM showed the immunolocalization of AhR mainly in the cytoplasm (Fig. 2A–C). However, 55.9 ± 6.0% of cells cultured in CM + 10 μM BaP revealed the distribution of AhR both in the cytoplasm and the nucleus (Fig. 2E–G). Staining with no primary antibody did not reveal any positive reactions (Fig. 2D,H). Since *cytochrome P450 1A1* (*CYP1A1*), *cytochrome P450 1B1* (*CYP1B1*), and *aryl-hydrocarbon receptor repressor* (*AhRR*) were reported as the novel target genes of the AhR pathway (Mimura et al., 1999), we investigated gene expression in HPDLCs-2G, -2I, and HaCaT by quantitative RT-PCR analysis. After 24 h of BaP exposure, HaCaT showed respectable up-regulation of *CYP1A1* mRNA, consistent with previous studies [Wanner et al., 1995]. Its induction was also observed in HPDLCs-2G and -2I, however, its expression level was much lower than HaCaT (Fig. 2I). The *CYP1B1* mRNA expression was clearly increased in HaCaT treated with BaP, while it was slightly up-regulated in HPDLCs-2G and -2I (Fig. 2J). The *AhRR* mRNA level was significantly up-regulated in these cells cultured in CM + 1 μM BaP and CM + 10 μM BaP, compared to the cultures in CM (Fig. 2K).

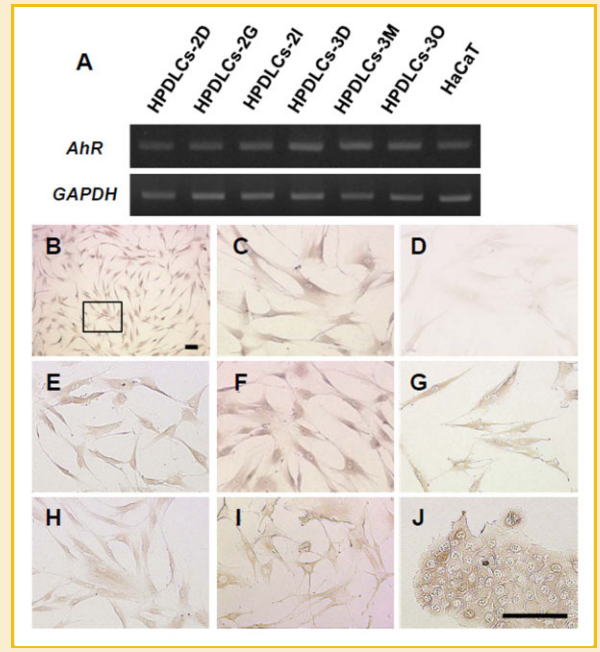

Fig. 1. Expression of AhR mRNA and AhR protein in HPDLCs. A: Semi-quantitative RT-PCR analysis of *AhR* mRNA expression in HPDLCs-2D, -2G, -2I, -3D, -3M, -3O, and HaCaT. Human *glyceraldehyde-3-phosphate dehydrogenase* (*GAPDH*) was used as an internal standard. B–J: Immunocytochemical staining images of anti-human AhR in HPDLCs-2G (B–D) and -2D (E), -2I (F), -3D (G), -3M (H), -3O (I), and HaCaT (J). C: Higher magnification images of the boxes in B. D: Staining images with no primary antibody as a negative control. Bars = 100 μm. Experiments were performed in duplicate. Representative data are shown.

INDUCTION OF MMP-1 EXPRESSION IN HPDLCs BY AHR PATHWAY ACTIVATION

Previous reports demonstrated the stimulation of MMP-1 expression through the activation of the AhR pathway in melanoma cells, vascular smooth muscle cells, and urothelial carcinoma cells [Villano et al., 2006; Meng et al., 2009]. Therefore, the expression of MMP-1 was examined in HPDLCs-2G, -2I, and HaCaT treated with

BaP. These cells, exposed to 1 and 10 μM BaP for 14 days, showed significant enhancement of *MMP-1* mRNA expression, compared to the untreated control cells (Fig. 3A). Next, this gene expression was further investigated in both HPDLCs treated with 10 μM BaP for 0, 14, or 28 days. The cells cultured in CM did not reveal a large change of *MMP-1* mRNA expression even if the culture period was extended, whereas the cells cultured in CM + 10 μM BaP exhibited up-regulation depending on the culture period (Fig. 3B,C). In addition, after 28 days of culture with 10 μM BaP, HPDLCs-2G, and -2I increased *MMP-1* mRNA expression to 4076.7 ± 35.6% and 2086.7 ± 15.1% of untreated control cells, respectively (Fig. 3B,C). Furthermore, ELISA analysis confirmed a marked increase in the expression of MMP-1 protein in HPDLCs cultured in CM + 10 μM BaP for 14 days (Fig. 3D).

SUPPRESSION OF COL-I AND α-SMA EXPRESSION IN HPDLCs BY AhR PATHWAY ACTIVATION

The expression of *COL-I* and *α-SMA* mRNAs was examined in HPDLCs-2G, -2I, and HaCaT treated with BaP. After 14 days of culture with 1 or 10 μM BaP, the expression of *COL-I* mRNA was distinctly decreased in HPDLCs-2G and HaCaT, while HPDLCs-2I showed no significant difference, compared to untreated control cells (Fig. 4A). The expression of *α-SMA* mRNA was markedly suppressed in HPDLCs-2G, -2I, and HaCaT in a dose-dependent manner (Fig. 4B). These gene expressions were further investigated in HPDLCs-2G and -2I exposed to 10 μM BaP for 0, 14, or 28 days. Both types of cells incubated in CM showed a tendency to increase *COL-I* mRNA expression as time advanced, while cells incubated in CM + 10 μM BaP demonstrated the suppression of this gene expression (Fig. 4C,D). In addition, after 28 days of culture with 10 μM BaP, HPDLCs-2G, and -2I significantly decreased *COL-I* mRNA expression to 3.4 ± 0.3% and 5.9 ± 0.4% of control untreated cells, respectively (Fig. 4C,D). Moreover, *α-SMA* mRNA expression was also suppressed in HPDLCs-2G and -2I treated with 10 μM BaP, compared to control untreated cells. After 14 days, HPDLCs-2G and -2I significantly decreased *α-SMA* mRNA expression to 39.6 ± 1.2% and 50.6 ± 3.7% of control untreated cells, respectively, while after 28 days, only HPDLCs-2G significantly suppressed its expression to 10.5 ± 0.5% of control untreated cells (Fig. 4E,F).

INDUCTION OF APOPTOSIS IN HPDLCs BY AhR PATHWAY ACTIVATION

To examine the effects of AhR pathway activation on cell proliferation of HPDLCs, direct cell count was performed in HPDLCs-2G and -2I. Both HPDLCs treated with BaP showed low proliferation in dose-dependent manner (Fig. 5A–C). At 7 days of culture, a significant reduction was found at CM + 10 μM BaP in HPDLCs-2G and -2I to 23.5 ± 2.0% and 20.6 ± 2.1% as compared to untreated control cells, respectively (Fig. 5B,C). To verify whether BaP-decreased cell proliferation exhibits the characteristics of apoptosis, flow cytometric analysis of double-staining with annexin V and PI was performed. After 3 h of culture, the cells cultured in CM showed a low percentage of annexin V positive cells (annexin V^+/PI^- and annexin V^+/PI^+) in HPDLCs-2G (0.8%) and -2I (1.1%; Fig. 5D), while treament with CM + 10 μM BaP increased the

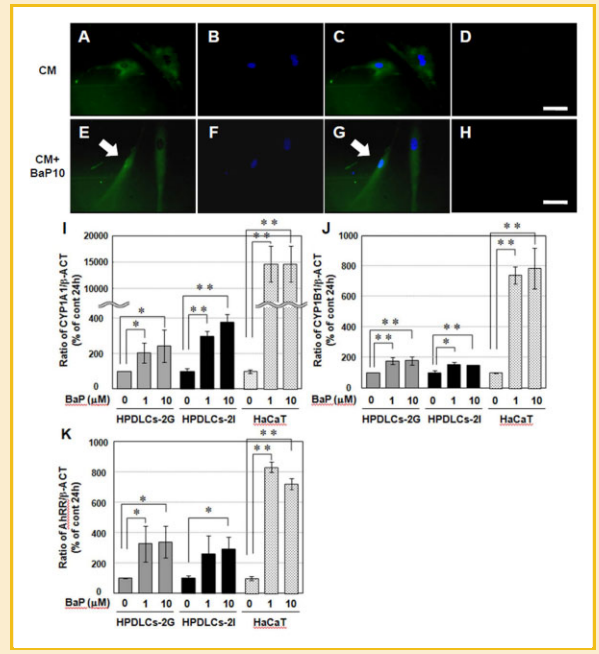

Fig. 2. Effects of BaP exposure on the expression of AhR and AhR ligand responsive genes in HPDLCs. HPDLCs-2G was cultured in CM (A–D) or CM + 10 μM BaP (CM + BaP10) (E–H) for 4 days. Fluorescence microscopic images of human AhR (A,E), DAPI (B,F), or merging of both stainings (C,G). Arrow shows the translocation of AhR from the cytoplasm to the nucleus. D,H: Staining images with no primary antibody as a negative control. Bars = 50 μm. I–K: Expression of *CYP1A1* (I), *CYP1B1* (J), and *AhRR* (K) mRNA was investigated using quantitative RT-PCR. HPDLCs-2G, -2I, and HaCaT were cultured in CM, CM + 1 μM BaP, or CM + 10 μM BaP for 24 h. Human *β-actin* (*β-ACT*) was used as an internal standard. Experiments were performed in triplicate. Representative data are shown. $^*P < 0.05$, $^{**}P < 0.01$.

percentage of annexin V positive cells in HPDLCs-2G (85.7%) and -2I (84.6%). In addition, the annexin V^+/PI^- fraction was highest in HPDLCs-2G (65.1%) and -2I (70.0%). After 24 h of culture in CM, few cells revealed an annexin V positive reaction in HPDLCs-2G (0.9%) and -2I (1.9%), whereas BaP treatment for 24 h increased the number of apoptotic cells in HPDLCs-2G (93.0%) and -2I (99.1%). Moreover, the annexin V^+/PI^+ population was highest in HPDLCs-2G (67.3%) and -2I (70.7%). A previous study reported that Bcl-2 family genes, such as *Bcl-2*, were the most effective anti-apoptotic regulators [Reed, 2000]. Therefore, the expression of *Bcl-2* mRNA was investigated in HPDLCs-2G and -2I treated with 10 μM BaP for 20, 40, or 60 min. A significant reduction of *Bcl-2* mRNA expression was observed in the culture with BaP in both HPDLC-2G (40 and 60 min) and -2I (20 and 40 min), compared to untreated control cells (Fig. 5E,F). We further analyzed apoptotic cell death focusing on activated caspase-3/7 using fluorescent labeled compound. Caspase-3/7 has been reported to be responsible for the execution of apoptosis by cleaving many different types of proteins [Slee et al., 2001]. After 24 h of culture in CM, HPDLCs-2G and -2I did not show any positive reactions for activated caspase-3/7, however, many cells cultured in CM + 10 μM BaP were stained positively for this enzyme (Fig. 5G). Our data clearly demonstrated the localization of activated caspase-3/7 in the nuclei of apoptotic HPDLCs.

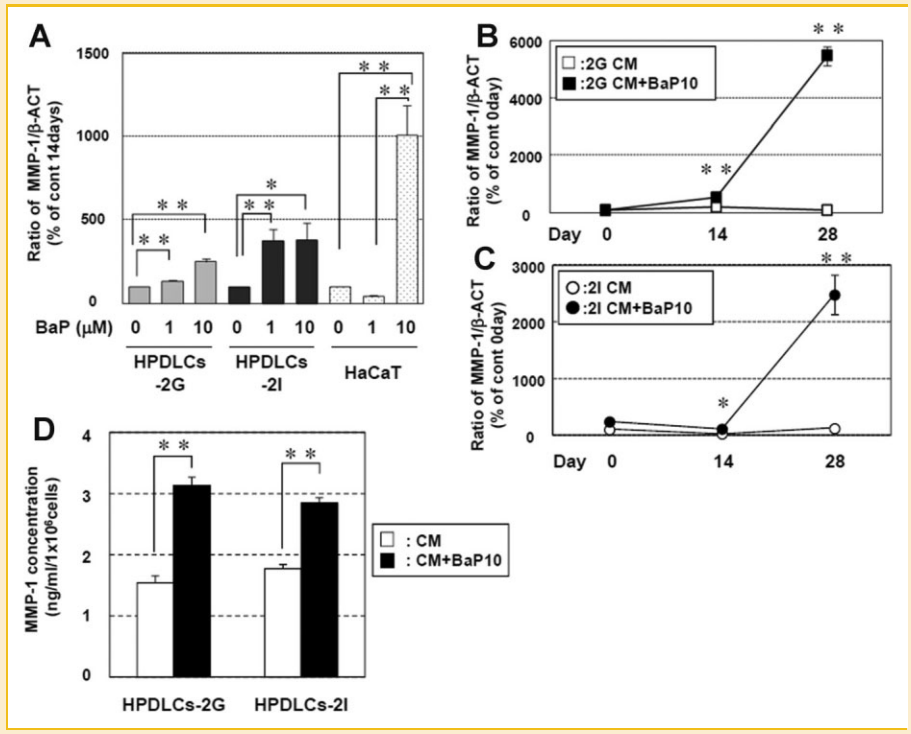

Fig. 3. Effects of BaP exposure on *MMP-1* mRNA expression and MMP-1 production in HPDLCs. A–C: Expression of *MMP-1* mRNA was investigated using quantitative RT-PCR. A: HPDLCs-2G, -2I, and HaCaT were cultured in CM, CM + 1 μM BaP, or CM + 10 μM BaP for 14 days. HPDLCs-2G (B) and -2I (C) were incubated in CM (□ or ○) or CM + 10 μM BaP (■ or ●) for 0, 14, or 28 days. D: MMP-1 concentration in condition medium of HPDLCs-2G and -2I cultured in CM or CM + 10 μM BaP for 14 days. Experiments were performed in triplicate. Representative data are shown. $^{*}P < 0.05$, $^{**}P < 0.01$

DISCUSSION

Previous reports have demonstrated the toxic effects of AhR ligands on various tissues including tooth and hard-tissue [Alaluusua and Lukinmaa, 2000; Jan and Vrbic, 2000; Kattainen et al., 2001; Partanen et al., 2004]. In addition, Shimizu et al. [1992] indicated there is a close relationship between orally ingested HAH and PDL tissue destruction, however, the particular effects of the ligand-activated AhR pathway on PDL tissue remain unclear. In this study, we suggest that AhR pathway activation induces the expression of disordered ECM remodeling-related molecules and apoptosis in two different HPDLCs; that is, HPDLCs-2G and -2I.

In our current study, *AhR* mRNA and AhR protein expression were confirmed in HPDLCs-2D, -2G, -2I, -3D, -3M, -3O, and HaCaT. To our knowledge, this is the first study to report AhR expression in HPDLCs. Moreover, incubation of HPDLCs with BaP resulted in a shift of AhR from cytosolic localization to cytosolic/nuclear distribution. A previous study reported that in the absence of ligand, AhR was found in the cytosol in a complex with several proteins such as HSP90, XAP, ARA9, and AIP, while after ligand binding, AhR moved to the nucleus and dimerized with ARNT [Rowlands and Gustafsson, 1997]. In addition, BaP treatment induced the up-regulation of *CYP1A1*, *CYP1B1*, and *AhRR* mRNA expression in HPDLCs-2G, -2I, and HaCaT. AhR controls the induction of cytochrome P450s in response to the presence of HAH and PAH; the AhR-ARNT dimer binds to a xenobiotic responsive element (XRE) and initiates the transcription of cytochrome P450s [Ma, 2007]. AhRR belongs to a bHLH/PAS protein family and acts as a negative feedback modulator. The transcription of AhRR is induced by the AhR-ARNT dimer through binding to XRE [Karchner et al., 2002]. These results suggested that BaP treatment induced the translocation of AhR into the nucleus and the expression of AhR responsive genes in HPDLCs. A previous report showed that *CYP1A1* and *CYP1B1* mRNA expression was induced by similar compounds [Bhattacharyya et al., 1995]. In HaCaT, both genes were considerably up-regulated by BaP. HPDLCs-2G and -2I also showed the induction of both genes, but the induction level of *CYP1B1* mRNA was quite slight. Moreover, their increase was much lower than that of HaCaT. Murray et al. [2001] reported that the expression patterns of *CYP1A1* gene differs from that of *CYP1B1* in a lot of tissues and suggested that there are considerable differences regarding the regulation, metabolic specificity, and tissue-specific expression of both genes. Moreover, Uno et al. [2004] suggested that CYP1A1 is important in BaP detoxification and CYP1B1 is responsible for metabolic activation of BaP, despite their close relationship. These findings indicated that PDL tissue may be subject to the toxic effects of HAH and PAH with the low detoxification and metabolic activation.

In PDL tissue, MMP-1 is considered to be crucial for tissue remodeling due to its function in degrading COL-I and -III [Kerrigan et al., 2000]. In our present study, BaP exposure promoted the extreme expression of *MMP-1* mRNA and MMP-1 protein in HPDLCs-2G and -2I. This result was supported by previous findings that the AhR pathway activated by TCDD increased MMP-1

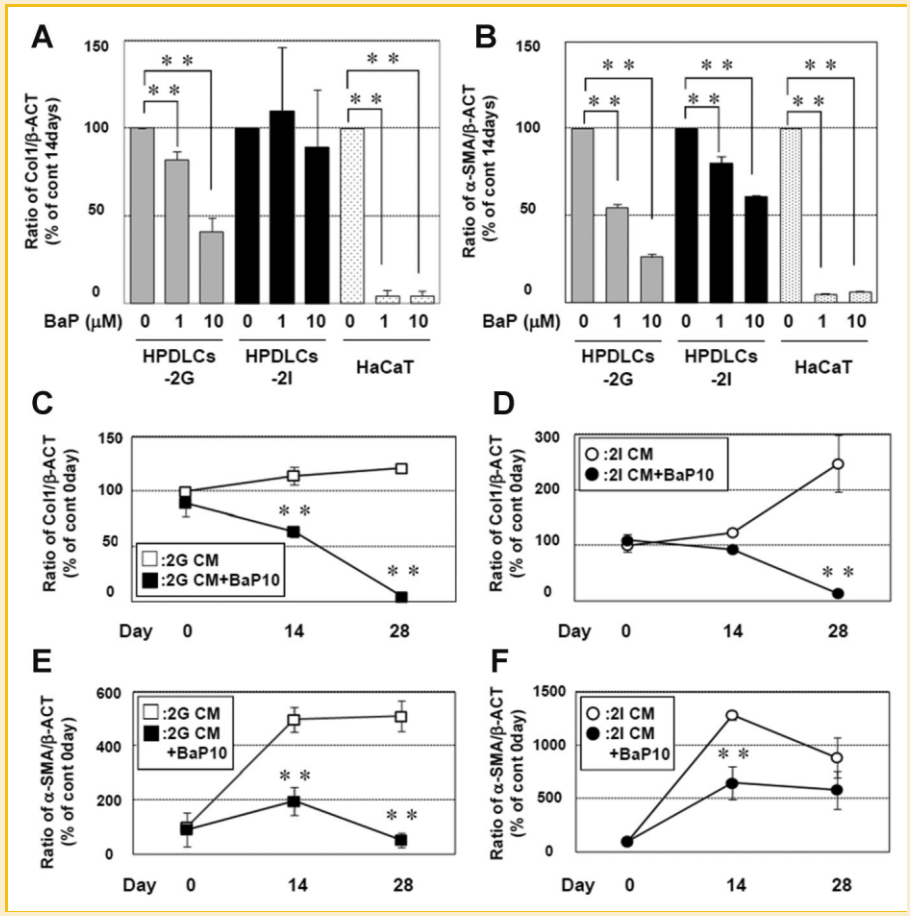

Fig. 4. Effects of BaP exposure on *Col-I* and *α-SMA* mRNA expression in HPDLCs. Expression of *Col-I* (A,C,D) and *α-SMA* (B,E,F) mRNA was investigated by using quantitative RT-PCR. A,B: HPDLCs-2G, -2I, and HaCaT were cultured in CM, CM + 1 μM BaP, or CM + 10 μM BaP for 14 days. HPDLCs-2G (C,E) and -2I (D,F) were incubated in CM (□ or ○) or CM + 10 μM BaP (■ or ●) for 0, 14, or 28 days. Experiments were performed in triplicate. Representative data are shown. $^{**}P < 0.01$.

expression in keratinocytes and melanoma cells [Murphy et al., 2004]. In addition, inappropriate expression of MMP-1 is involved in several pathologies such as rheumatoid arthritis [Maeda et al., 1995], Alzheimer's disease [Leake et al., 2000], and tumor metastasis [Ishii et al., 2003]. Interestingly, remarkable up-regulation of MMP-1 expression was exhibited in PDL cells in patients with chronic periodontal diseases [Reynolds et al., 1994]. *Prevotella intermedia*, a major periodontal pathogen that plays an important role in the development of periodontitis, markedly promoted MMP-1 expression in PDL cells [Guan et al., 2009]. These results suggested that the increased MMP-1 via AhR pathway activation would have a close contribution to pathologic degradation of PDL tissue.

COL-I is known as the connective tissue protein central in tendon, ligament, bone, and PDL tissue [Becker et al., 1991]. In PDL tissue, it is synthesized in approximately 99% of PDL cells [Connor et al., 1983], whereas HPDLCs-2G and -2I exposed to BaP for 28 days reduced *COL-I* mRNA to <10% in comparison to the untreated control cells. Sodek and Limeback [1979] revealed the continuous and rapid collagen turnover in PDL tissue, and Perera and Tonge [1981] focused attention on collagen synthesis of PDL cells as an index of metabolic turnover. Therefore, AhR pathway activation might prevent collagen turnover in PDL tissue via the suppression of COL-I synthesis in PDL cells. Moreover, a marked decrease of *α-SMA* mRNA expression was also exhibited in HPDLCs-2G and -2I exposed to BaP. α-SMA is known as the most reliable marker of myofibroblasts. Previous reports suggested the involvement of myofibroblasts in ECM synthesis and in force generation, which promoted ECM reorganization and wound healing [Tomasek et al., 2002]. Arora and McCulloch [1994] demonstrated that PDL fibroblasts with a high remodeling capacity also strongly expressed α-SMA. Interestingly, the close relationship between connective tissue regeneration and COL-I or α-SMA expression has been previously demonstrated. Sculean et al. [2002] revealed strong expression of COL-I in regenerating PDL tissue compared to normal PDL tissue. Agarwal et al. [2006] showed the promotion of α-SMA expression in healing fibroblasts in collateral ligaments. Olaso et al. [2011] revealed a delay of cutaneous wound healing with the suppression of α-SMA expression in discoidin domain receptor 2 knockout mice. These results suggested that AhR pathway activation in PDL tissue would provoke PDL tissue destruction and induce inappropriate remodeling through the decrease of COL-I and α-SMA expression.

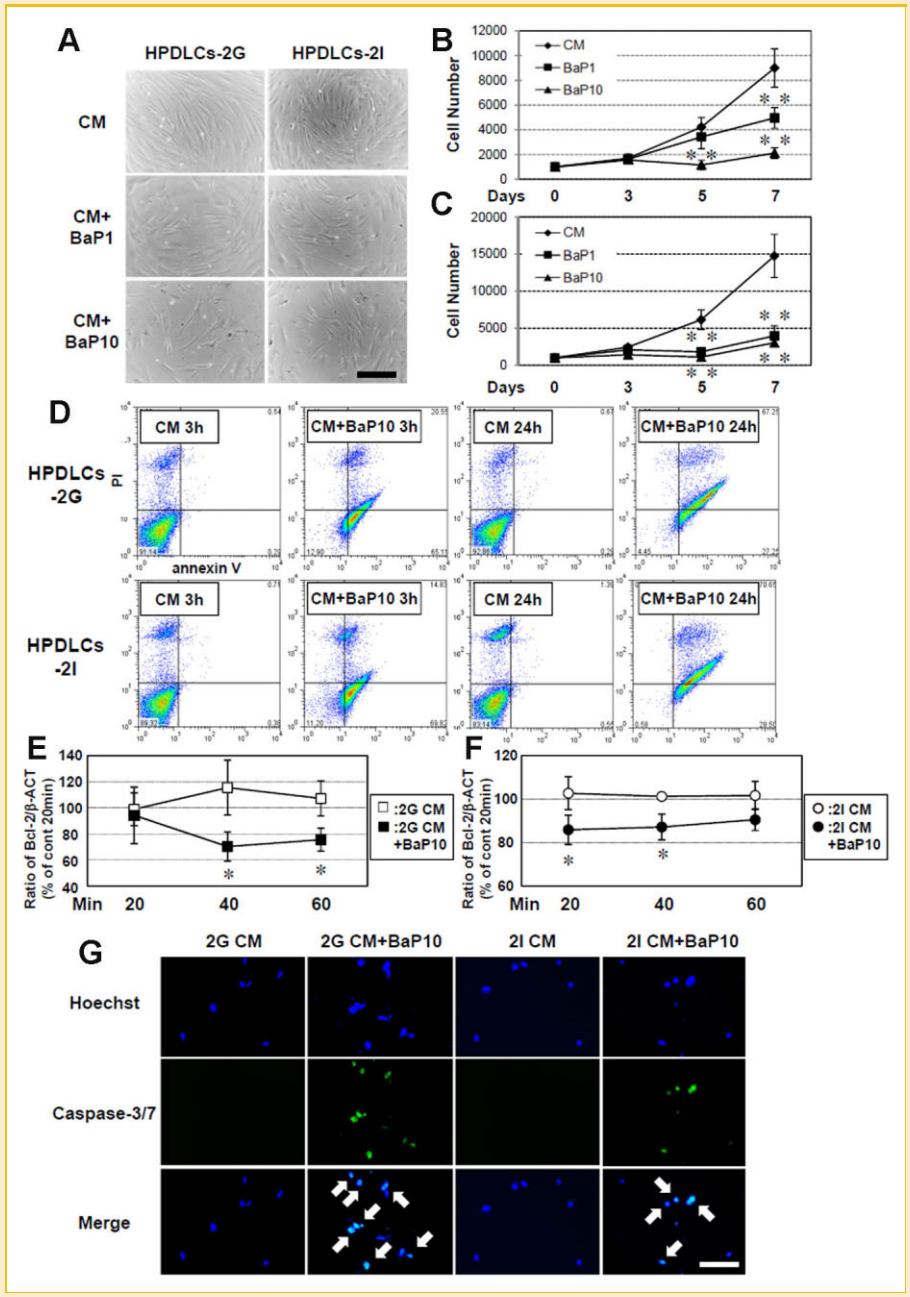

Fig. 5. Apoptotic effects of BaP exposure on HPDLCs. A: Phase-contrast microscopic images of HPDLCs-2G and -2I cultured in CM, CM + 1 μM BaP, or CM + 10 μM BaP for 7 days. B,C: Cell number of HPDLCs-2G (B) and -2I (C) incubated in CM (◆), CM + 1 μM BaP (■), or CM + 10 μM BaP (▲) for 0, 3, 5, or 7 days. D: Flow cytometric analysis of the expression of annexin V and PI. HPDLCs-2G and -2I were cultured in CM or CM+ 10 μM BaP for 3 or 24 h. E,F: Expression of *Bcl-2* mRNA was investigated by using quantitative RT-PCR. HPDLCs-2G (E) and -2I (F) were cultured in CM (□ or ○) or CM + 10 μM BaP (■ or ●) for 20in, 40, or 60 min. G: Fluorescence microscopic images of Hoechst (blue), caspase-3/7 (green), or merging of both stainings in HPDLCs-2G and -2I. These cells were cultured in CM or CM + 10 μM BaP for 24 h. Arrows show double-positive cells expressing activated caspase-3/7 that is localized in nuclei. Bar = 100 μm. Experiments were performed in quadruplicate. Representative data are shown. $^{*}P < 0.05$, $^{**}P < 0.01$

Transforming growth factor β1 (TGFβ1), a member of the TGFβ superfamily, was reported to induce COL-I and α-SMA expression in myofibroblasts (Desmouliere et al., 1993). Our recent study demonstrated high expression of TGFβ1 in PDL cells in vivo and in vitro [Fujii et al., 2010]. To examine the involvement of TGFβ signaling in AhR-induced COL-I and α-SMA suppression, we investigated the expression of *TGFβ1* mRNA in HPDLCs-2G and -2I treated with BaP, but did not confirm any significant differences (data not shown). Abbott and Birnbaum [1990] demonstrated that AhR activation by TCDD reduced TGFβ1 expression in epithelial and mesenchymal cells. On the other hand, Gramatzki et al. [2004] showed that 3-methylcholanthrene, a member of PAH, did not influence TGFβ1 expression in glioma cells. Thus, AhR activation may regulate TGFβ signaling pathways in a cell type-specific

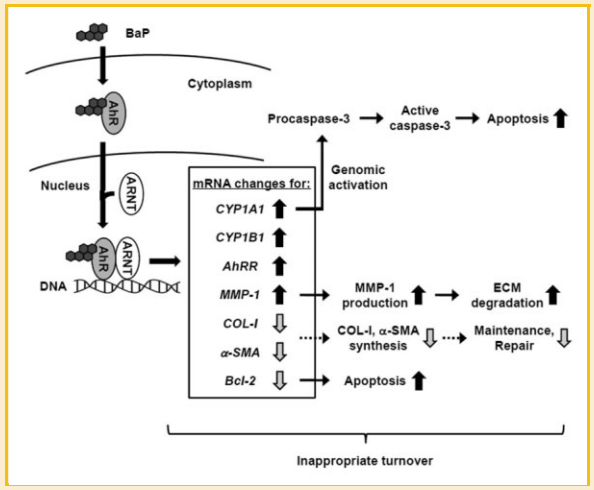

Fig. 6. A schematic model for the effects of AhR pathway activation on HPDLCs. After BaP binds to the cytosolic receptor protein AhR, the ligand-bound AhR translocates to the nucleus, dimerizing with ARNT. This complex alters the expression of its target genes [Rowlands and Gustafsson, 1997]. The data presented in this study suggested that overactivity of the AhR pathway may induce inappropriate turnover in PDL tissue through at least three mechanisms: (i) AhR pathway activation increases the expression of *MMP-1* mRNA and MMP-1 protein and promotes ECM degradation; (ii) AhR pathway activation decreases the expression of *COL-I* and *a-SMA* mRNA and may impair maintaining or repairing PDL tissue via the suppression of COL-I and a-SMA synthesis; and (iii) AhR pathway activation decreases the expression of *Bcl-2* mRNA, activates caspase-3, and induces apoptosis.

manner and furthermore the suppression of *COL-I* and *α-SMA* mRNA expression by AhR activation may be independent of the TGFβ signaling pathway in PDL cells.

Apoptosis is an evolutionarily conserved form of cell suicide. AhR ligands were previously reported to induce apoptotic cell death in several types of cells such as thymocytes, ovarian germ cells, liver epithelial cells, and chondrocytes [Yang and Lee, 2010]. In addition, the AhR-deficient mice were resistant to TCDD-induced apoptosis [Fernandez-Salguero et al., 1996]. These results suggested the contribution of the AhR pathway as the mediator of apoptotic effects on various tissues. In this study, we demonstrated BaP-induced apoptosis of HPDLCs-2G and -2I through a decrease in total cell number and an increase in the percentage of annexin V-positive cells. Annexin V binds to phosphatidylserine, which is translocated from the inner surface of the plasma membrane to the outer cell surface early in the process of apoptosis [Martin et al., 1995]. We found that the highest fractions of annexin V^+/PI^-, implying early apoptosis, appeared in 3 h cultures treated with BaP, while the fraction of annexin V^+/PI^+, implying late apoptosis, were increased in 24 h cultures with BaP. In addition, we observed the suppression of the most effective antiapoptotic gene, *Bcl-2*, in both HPDLCs exposed to BaP. In support of our findings, previous reports showed BaP-induced Bcl-2 reduction in Burkitt's lymphoma cells [Salas and Burchiel, 1998], hepatoma cells [Ko et al., 2004], and lung fibroblasts [Jiang et al., 2012]. Caspases are key enzymes in apoptosis and their activation is a cascade of elemental reactions to cell death. Caspase-3 and -7, so-called effector caspases, play a pivotal role in initiating apoptosis. Lei et al. [1998] suggested that caspase-3 has been engaged in caspase-dependent apoptosis of BaP in mouse Hepa1c1c7 hepatoma cells. Furthermore, Tampio et al. [2008] revealed caspase-7 activation after BaP treatment of human MCF-7 breast adenocarcinoma cells. Consistently, with these results, our data demonstrated an increase in activated caspase-3/7- positive cells in HPDLCs-2G and -2I treated with BaP. In addition, activated caspase-3/7 is mainly localized in the nuclei of BaP-treated HPDLCs. Kamada et al. [2005] reported nuclear localization of activated caspase-3 but not caspase-7 in apoptotic human hepatocellular carcinoma cells. These results indicated that AhR pathway activation may induce PDL cell apoptosis by the reduction of *Bcl-2* mRNA expression and the activation of caspase-3. Our present study showed the increase of *CYP1A1* and *CYP1B1* mRNA in HPDLCs-2G and -2I cultured for short period, namely 24 h with BaP. CYP1A1 has been reported to play important roles in BaP-induced apoptosis because α-naphthoflavone, an inhibitor of CYP1A1 activity, significantly reduced BaP-induced apoptosis [Solhaug et al., 2005]. In contrast, 2, 3′, 4, 5′-tetramethoxystilbene and pyrene, CYP1B1-specific inhibitors, couldn't suppress BaP-induced apoptosis. Furthermore, Kim et al. [2007] previously reported the involvement of not CYP1B1 but CYP1A1 in BaP-induced caspase-3 activation in Hepa1c1c7 cells and human RL95-2 endometrial cancer cells. These results indicated that BaP-bound AhR may activate caspase-3 through the genomic pathway involved in the fast transcriptional regulation of *CYP1A1* mRNA in HPDLCs.

In summary, we presented AhR expression in HPDLCs-2G and -2I and confirmed its activation induced by BaP binding. BaP exposure altered the expression of ECM-related molecules, MMP-1, Col-I, and α-SMA and induced apoptosis in both HPDLCs. Overactivity of the AhR pathway may induce inappropriate turnover via disordered ECM remodeling and apoptosis in PDL tissue. A proposed model for the effects of AhR pathway activation on HPDLCs is shown in Figure 6. Our findings may help to establish new therapy for AhR-induced periodontal diseases. In future studies, the mechanisms of signaling in the AhR pathway in PDL cells need to be elucidated.

ACKNOWLEDGMENTS

This work was financially supported by Grants-in-Aid for Scientific Research (Project Nos. 21390510, 21791942, 22390359, 23659890, and 23689077) from the Japan Society for the Promotion of Science.

REFERENCES

Abbott BD, Birnbaum LS. 1990. TCDD-induced altered expression of growth factors may have a role in producing cleft palate and enhancing the incidence of clefts after coadministration of retinoic acid and TCDD. Toxicol Appl Pharmacol 106:418–432.

Agarwal C, Britton ZT, Alaseirlis DA, Li Y, Wang JHC. 2006. Healing and normal fibroblasts exhibit differential proliferation, collagen production, a-SMA expression, and contraction. Ann Biomed Eng 34:653–659.

Alaluusua S, Lukinmaa PL. 2000. Developmental dental toxicity of dioxin and related compounds—A review. Int Dent J 56:323–331.

Alvares O, Klebe R, Grant G, Cochran DL. 1995. Growth factor effects on the expression of collagenase and TIMP-1 in periodontal ligament cells. J Periodontol 66:552–558.

Arora PD, McCulloch CA. 1994. Dependence of collagen remodelling on alpha-smooth muscle actin expression by fibroblasts. J Cell Physiol 159:161–175.

Becker J, Schuppan D, Rabanus JP, Rauch R, Niechoy U, Gelderblom HR. 1991. Immunoelectron microscopic localization of collagens type I, V, VI and of procollagen type III in human periodontal ligament and cementum. J Histochem Cytochem 39:103–110.

Bhattacharyya K, Brake P, Eltom SE, Otto S, Jefcoate CR. 1995. Identification of a rat adrenal cytochrome P450 active in polycyclic hydrocarbon metabolism as rat CYP1B1. Demonstration of a unique tissue-specific pattern of hormonal and aryl hydrocarbon receptor-linked regulation. J Biol Chem 270:11595–11602.

Boukamp P, Petrussevska RT, Breitkreutz D, Hornung J, Markham A, Fusenig NE. 1988. Normal keratinization in a spontaneously immortalized aneuploid human keratinocyte cell line. J Cell Biol 106:761–771.

Butler WT, Birkedal-Hansen H, Beegle WF, Taylor RE, Chung E. 1975. Proteins of the periodontium. Identification of collagens with the [alpha1(I)]2alpha2 and [alpha1(III)]3 structures in bovine periodontal ligament. J Biol Chem 250:8907–8912.

Carnes DL, Maeder CL, Graves DT. 1997. Cells with osteoblastic phenotypes can be explanted from human gingiva and periodontal ligament. J Periodontol 68:701–707.

Connor NS, Aubin JE, Sodek J. 1983. Independent expression of type I collagen and fibronectin by normal fibroblast-like cells. J Cell Sci 63:233–244.

Desmouliere A, Geinoz A, Gabbiani F, Gabbiani G. 1993. Transforming growth factor-beta 1 induces alpha-smooth muscle actin expression in granulation tissue myofibroblasts and in quiescent and growing cultured fibroblasts. J Cell Biol 122:103–111.

Desmouliere A, Chaponnier C, Gabbiani G. 2005. Tissue repair, contraction, and the myofibroblast. Wound Repair Regen 13:7–12.

Fernandez-Salguero PM, Hilbert DM, Rudikoff S, Ward JM, Gonzalez FJ. 1996. Aryl-hydrocarbon receptor-deficient mice are resistant to 2,3,7,8-tetrachlorodibenzo-*p*-dioxin-induced toxicity. Toxicol Appl Pharmacol 140:173–179.

Freeman E. 1994. Peridontium. In: Ten Cate AR, editor. Oral histology: Development, structure, and function. St. Louis: Mosby. pp 276–312.

Fujii S, Maeda H, Wada N, Kano Y, Akamine A. 2006. Establishing and characterizing human periodontal ligament fibroblasts immortalized by SV40T-antigen and hTERT gene transfer. Cell Tissue Res 324:117–125.

Fujii S, Maeda H, Wada N, Tomokiyo A, Saito M, Akamine A. 2008. Investigating a clonal human periodontal ligament progenitor/stem cell line in vitro and in vivo. J Cell Physiol 215:743–749.

Fujii S, Maeda H, Tomokiyo A, Monnouchi S, Hori K, Wada N, Akamine A. 2010. Effects of TGF-β1 on the proliferation and differentiation of human periodontal ligament cells and a human periodontal ligament stem/progenitor cell line. Cell Tissue Res 342:233–242.

Galis ZS, Sukhova GK, Lark MW, Libby P. 1994. Increased expression of matrix metalloproteinases and matrix degrading activity in vulnerable regions of human atherosclerotic plaques. J Clin Invest 94:2493–2503.

Gramatzki D, Pantazis G, Schittenhelm J, Tabatabai G, Köhle C, Wick W, Schwarz M, Weller M, Tritschler I. 2004. Aryl hydrocarbon receptor inhibition downregulates the TGF-beta/Smad pathway in human glioblastoma cells. Toxicology 199:35–46.

Gu Y, Hamajima N, Ihara Y. 2000. Neurofibrillary tangle-associated collapsin response mediator protein-2 (CRMP-2) is highly phosphorylated on Thr-509, Ser-518, and Ser-522. Biochemistry 39:4267–4275.

Guan SM, Shu L, Fu SM, Liu B, Xu XL, Wu JZ. 2009. Prevotella intermedia upregulates MMP-1 and MMP-8 expression in human periodontal ligament cells. FEMS Microbiol Lett 299:214–222.

Ikuta T, Kobayashi Y, Kawajiri K. 2004. Cell density regulates intracellular localization of aryl hydrocarbon receptor. J Biol Chem 279:19209–19216.

Ishii Y, Ogura T, Tatemichi M, Fujisawa H, Otsuka F, Esumi H. 2003. Induction of matrix metalloproteinase gene transcription by nitric oxide and mechanisms of MMP-1 gene induction in human melanoma cell lines. Int J Cancer 103:161–168.

Jan J, Vrbic V. 2000. Polychlorinated biphenyls cause developmental enamel defects in children. Caries Res 34:469–473.

Jiang Y, Rao K, Yang G, Chen X, Wang Q, Liu A, Zheng H, Yuan J. 2012. Benzo(a)pyrene induces p73 mRNA expression and necrosis in human lung adenocarcinoma H1299 cells. Environ Toxicol 27:202–210.

Kamada S, Kikkawa U, Tsujimoto Y, Hunter T. 2005. Nuclear translocation of caspase-3 is dependent on its proteolytic activation and recognition of a substrate-like protein(s). J Biol Chem 280:857–860.

Karchner SI, Franks DG, Powell WH, Hahn ME. 2002. Regulatory interactions among three members of the vertebrate aryl hydrocarbon receptor family: AHR repressor, AHR1, and AHR2. J Biol Chem 277:6949–6959.

Kattainen H, Tuukkanen J, Simanainen U, Tuomisto JT, Kovero O, Lukinmaa PL, Alaluusua S, Tuomisto J, Viluksela M. 2001. In utero/lactational 2,3,7,8-tetrachlorodibenzo-*p*-dioxin exposure impairs molar tooth development in rats. Toxicol Appl Pharmacol 174:216–224.

Kerrigan JJ, Mansell JP, Sandy JR. 2000. Matrix turnover. J Orthod 27:227–233.

Kim JY, Chung JY, Park JE, Lee SG, Kim YJ, Cha MS, Han MS, Lee HJ, Yoo YH, Kim JM. 2007. Benzo[a]pyrene induces apoptosis in RL95-2 human endometrial cancer cells by cytochrome P450 1A1 activation. Endocrinology 148:5112–5122.

Ko CB, Kim SJ, Park C, Kim BR, Shin CH, Choi S, Chung SY, Noh JH, Jeun JH, Kim NS, Park R. 2004. Benzo(a)pyrene-induced apoptotic death of mouse hepatoma Hepa1c1c7 cells via activation of intrinsic caspase cascade and mitochondrial dysfunction. Toxicology 199:35–46.

Leake A, Morris CM, Whateley J. 2000. Brain matrix metalloproteinase 1 levels are elevated in Alzheimer's disease. Neurosci Lett 291:201–203.

Lei W, Yu R, Mandlekar S, Kong AN. 1998. Induction of apoptosis and activation of interleukin 1β-converting enzyme/Ced-3 protease (caspase-3) and c-Jun NH2-terminal kinase 1 by benzo(a)pyrene. Cancer Res 58:2102–2106.

Lekic P, Rojas J, Birek C, Tenenbaum H, McCulloch CA. 2001. Phenotypic comparison of periodontal ligament cells in vivo and in vitro. J Periodontal Res 36:71–79.

Loro L, Vintermyr OK, Johannessen AC. 2005. Apoptosis in normal and diseased oral tissues. Oral Dis 11:274–287.

Ma Q. 2007. Aryl hydrocarbon receptor degradation-promoting factor (ADPF) and the control of the xenobiotic response. Mol Interv 7:133–137.

Maeda S, Sawai T, Uzuki M, Takahashi Y, Omoto H, Seki M, Sakurai M. 1995. Determination of interstitial collagenase (MMP-1) in patients with rheumatoid arthritis. Ann Rheum Dis 54:970–975.

Maeda H, Tomokiyo A, Koori K, Monnouchi S, Fujii S, Wada N, Kono K, Yamamoto N, Saito T, Akamine A. 2011. An in vitro evaluation of two resin-based sealers on proliferation and differentiation of human periodontal ligament cells. Int Endod J 44:425–431.

Martin SJ, Reutelingsperger CP, McGahon AJ, Rader JA, van Schie RC, LaFace DM, Green DR. 1995. Early redistribution of plasma membrane phosphatidylserine is a general feature of apoptosis regardless of the initiating stimulus: Inhibition by overexpression of Bcl-2 and Abl. J Exp Med 182:1545–1556.

Meng D, Lv DD, Zhuang X, Sun H, Fan L, Shi XL, Fang J. 2009. Benzo[a]-pyrene induces expression of matrix metalloproteinases and cell migration and invasion of vascular smooth muscle cells. Toxicol Lett 184:44–49.

Mimura J, Ema M, Sogawa K, Fujii-Kuriyama Y. 1999. Identification of a novel mechanism of regulation of Ah (dioxin) receptor function. Genes Dev 13:20–25.

Murphy KA, Villano CM, Dorn R, White LA. 2004. Interaction between the aryl hydrocarbon receptor and retinoic acid pathways increases matrix metalloproteinase-1 expression in keratinocytes. J Biol Chem 279:25284–25293.

Murray GI, Melvin WT, Greenlee WF, Burke MD. 2001. Regulation, function, and tissue-specific expression of cytochrome P450 CYP1B1. Annu Rev Pharmacol Toxicol 41:297–316.

Nebert DW, Roe AL, Dieter MZ, Solis WA, Yang Y, Dalton TP. 2000. Role of the aromatic hydrocarbon receptor and [Ah] gene battery in the oxidative stress response, cell cycle control, and apoptosis. Biochem Pharmacol 59: 65–85.

Nemoto T, Kajiya H, Tsuzuki T, Takahashi Y, Okabe K. 2010. Differential induction of collagens by mechanical stress in human periodontal ligament cells. Arch Oral Biol 55:981–987.

Olaso E, Lin HC, Wang LH, Friedman SL. 2011. Impaired dermal wound healing in discoidin domain receptor 2-deficient mice associated with defective extracellular matrix remodeling. Fibrogenesis Tissue Repair 4:5.

Partanen AM, Kiukkonen A, Sahlberg C, Alaluusua S, Thesleff I, Pohjanvirta R, Lukinmaa PL. 2004. Developmental toxicity of dioxin to mouse embryonic teeth in vitro: Arrest of tooth morphogenesis involves stimulation of apoptotic program in the dental epithelium. Toxicol Appl Pharmacol 194:24–33.

Perera KA, Tonge CH. 1981. Metabolic turnover of collagen in the mouse molar periodontal ligament during tooth eruption. J Anat 133:359–370.

Pohjanvirta R, Tuomisto J. 1994. Short-term toxicity of 2,3,7,8-tetrachlorodibenzo-*p*-dioxin in laboratory animals: Effects, mechanisms, and animal models. Pharmacol Rev 46:483–549.

Reed JC. 2000. Mechanisms of apoptosis. Am J Pathol 157:1415–1430.

Reynolds JJ, Hembry RM, Meikle MC. 1994. Connective tissue degradation in health and periodontal disease and the roles of matrix metalloproteinases and their natural inhibitors. Adv Dent Res 8:312–319.

Rowlands JC, Gustafsson JA. 1997. Aryl hydrocarbon receptor-mediated signal transduction. Crit Rev Toxicol 27:109–134.

Salas VM, Burchiel SW. 1998. Apoptosis in Daudi human B cells in response to benzo[a]pyrene and benzo[a]pyrene-7,8-dihydrodiol. Toxicol Appl Pharmacol 151:367–376.

Sculean A, Junker R, Donos N, Berakdar M, Brecx M, Dünker N. 2002. Immunohistochemical evaluation of matrix molecules associated with wound healing following regenerative periodontal treatment in monkeys. Clin Oral Investig 6:175–182.

Shimizu K, Nakata S, Murakami T, Tamari K, Takahama Y, Akamine A, Aono M. 1992. Long-term occlusal guidance of a severely intoxicated patient with yusho (PCB poisoning): A case report. Am J Orthod Dentofacial Orthop 101:393–402.

Shimono M, Ishikawa T, Ishikawa H, Matsuzaki H, Hashimoto S, Muramatsu T, Shima K, Matsuzaka K, Inoue T. 2003. Regulatory mechanisms of periodontal regeneration. Microsc Res Technol 60:491–502.

Skalli O, Ropraz P, Trzeciak A, Benzonana G, Gillessen D, Gabbiani G. 1986. A monoclonal antibody against α-smooth muscle actin: A new probe for smooth muscle differentiation. J. Cell Biol 103:2787–2796.

Slee EA, Adrain C, Martin SJ. 2001. Executioner caspase-3, -6, and -7 perform distinct, non-redundant roles during the demolition phase of apoptosis. J Biol Chem 276:7320–7326.

Sodek J, Limeback HF. 1979. Comparison of the rates of synthesis, conversion, and maturation of type I and type III collagens in rat periodontal tissues. J Biol Chem 254:10496–10502.

Solhaug A, Øvrebø S, Mollerup S, Låg M, Schwarze PE, Nesnow S, Holme JA. 2005. Role of cell signaling in B[a]P-induced apoptosis: Characterization of unspecific effects of cell signaling inhibitors and apoptotic effects of B[a]P metabolites. Chem Biol Interact 151:101–119.

Tampio M, Loikkanen J, Myllynen P, Mertanen A, Vähäkangas KH. 2008. Benzo(a)pyrene increases phosphorylation of p53 at serine 392 in relation to p53 induction and cell death in MCF-7 cells. Toxicol Lett 178:152–159.

Tomasek JJ, Gabbiani G, Hinz B, Chaponnier C, Brown RA. 2002. Myofibroblasts and mechano-regulation of connective tissue remodelling. Nat Rev Mol Cell Biol 3:349–363.

Tomokiyo A, Maeda H, Fujii S, Wada N, Shima K, Akamine A. 2008. Development of a multipotent clonal human periodontal ligament cell line. Differentiation 76:337–347.

Uno S, Dalton TP, Derkenne S, Curran CP, Miller ML, Shertzer HG, Nebert DW. 2004. Oral exposure to benzo[a]pyrene in the mouse: Detoxication by inducible cytochrome P450 is more important than metabolic activation. Mol. Pharmacol 65:1225–1237.

Villano CM, Murphy KA, Akintobi A, White LA. 2006. 2,3,7,8-tetrachlorodibenzo-*p*-dioxin (TCDD) induces matrix metalloproteinase (MMP) expression and invasion in A2058 melanoma cells. Toxicol Appl Pharmacol 210:212–224.

Wanner R, Brömmer S, Czarnetzki BM, Rosenbach T. 1995. The differentiation-related upregulation of aryl hydrocarbon receptor transcript levels is suppressed by retinoic acid. Biochem Biophys Res Commun 209:706–711.

Wu J, Ramesh A, Nayyar T, Hood DB. 2003. Assessment of metabolites and AhR and CYP1A1 mRNA expression subsequent to prenatal exposure to inhaled benzo(a)pyrene. Int J Dev Neurosci 21:333–346.

Yang JH, Lee HG. 2010. 2,3,7,8-Tetrachlorodibenzo-*p*-dioxin induces apoptosis of articular chondrocytes in culture. Chemosphere 79:278–284.

Zhang JH, Dong Z, Chu L. 2010. Hydrogen sulfide induces apoptosis in human periodontium cells. J Periodontal Res 45:71–78.